MJFAS MALAYSIAN JOURNAL OF FUNDAMENTAL AND APPLIED SCIENCES
PRINT ISSN: 2289-5981 | ONLINE ISSN: 2289-599X

RESEARCH ARTICLE

Modified absorption attributes of neodymium doped magnesium-zinc-sulfophosphate glass

Nur Nabihah Yusof, Sib Krishna Ghoshal*, Muhammad Firdaus Omar

Physics Department, Faculty of Science, Universiti Teknologi Malaysia, 81310 UTM Johor Bahru, Johor, Malaysia

* *Corresponding author: sibkrishna@utm.my*

Article history
Received 16 February 2017
Accepted 4 July 2017

Abstract

Rare-earth doped glass systems with improved absorption and emission features are greatly demanding for diverse applications. In this endavour, selection of right glass host, modifier, rare earth ions with optimized composition is the key issue. This communication reports the conventional melt-quench synthesis of neodymium (Nd^{3+}) doped magnesium-zinc- sulfophosphate glass system of the form (60-*x*)P_2O_5-20MgO-20$ZnSO_4$-*x*Nd_2O_3 (*x* = 0, 0.5, 1, 1.5, 2.0 and 2.5 mol%). The influence of varying Nd^{3+} contents on the physical (density, molar volume, molar refractivity, refractive index and electronic polarizability) and absorption properties of the prepared glass system is determined. The amorphousity of the obtained samples is confirmed by XRD analysis. The glass refractive indices (ranged from 1.85 to 1.90) and densites (between 2.63 to 2.77 g.cm^{-3}) are found to increase with increasing concentration of Nd^{3+} ion. Furthermore, the energies associated with the direct and indirect optical transitions across the forbidden gap are observed to reduce with the increase of Nd^{3+} ion concentration. Meanwhile, the increase of Urbach energy with increasing Nd^{3+}doping is ascribed to the interaction of rare earth ions with the ligands of the glass network and subsequent transformation of weak bonds into defects. The room temperature UV–Vis-NIR spectra revealed eleven absorption band corresponding to the transitions from the ground state to various excited states of the Nd^{3+} ion. Incorporation of Nd^{3+} ion is discerned to enhance the glass absorbance appreciably together with the alteration of physical properties. Present findings may be beneficial for the advancement of Nd^{3+} ions doped magnesium-zinc-sulfophosphate glass system based photonic devices especially for infrared solid state laser.

***Keywords*:** Sulfophosphate glass, absorbance, ligand interaction, neodymium

INTRODUCTION

Glasses doped with rare-earth (RE) ions can be used as efficient lasers and optical amplifiers at various wavelengths, as frequency upconverters and color displays, for nonlinear optics and for integrated optics (Elan *et al.*, 2016). Among RE-doped oxide glasses, neodymium doped phosphate glasses have been largely investigated since neodymium emerged as one of the most efficient RE ions for solid-state lasers. The intense lasing emission ($^4F_{3/2}\rightarrow{}^4I_{11/2}$) of Nd^{3+} at metastable state is most useful (Ehrmann and Campbell, 2002). Meanwhile, phosphate glass has good solubility of RE ions (~5×10^{19} ions.cm^{-3} to 5×10^{20} ions.cm^{-3}) (Novais *et al.*, 2015), medium phonon energy, low nonlinear refractive index, and good spectroscopic host for Nd^{3+} ions compared with silicate glass host (Surana *et al.*, 2001; Hu *et al.*, 2014). Until now, neodymium-doped phosphate-based bulk glasses have been the most widely used laser glasses due to their superior optical properties (Miguel *et al.*, 2013).

Despite the excellent optical properties phosphate glass, their hygroscopic nature (Binnemans *et al.*, 1998; Reddy Prasad *et al.*, 2016) limits the applicability useless inhibited (Da *et al.*, 2010a; b; Ahmadi *et al.*, 2016a). Therefore, selection of appropriate glass compositions is crucial to achieve excellent optical performance together with their thermal, chemical and mechanical stability (Dorosz, 2008).

Among various modified, addition of alkali sulfides (e.g.. $ZnSO_4$) into the phosphate network bring advtanges in terms of lowering the glass transformation temperature (Da *et al.*, 2011), increasing the chemical durability (Thieme *et al.*, 2015), reducing the humidity attack at room temperature (Striepe *et al.*, 2012), diminishing the glass phonon energy (Griscom *et al.*, 2001) and enhancing the solubility of RE ions. Modifier oxides (e.g. MgO) inside the glass allows the strong luminescence and makes the glass system chemically more stable (Ahmadi *et al.*, 2016a; b). Actually, Zn ions provide strong ionic cross link between different phosphate anions and inhibit the hydration reaction (Elbashar *et al.*, 2016). Furthermore, the inclusion of alkaline-earth oxides such as MgO further improves the chemical durability of phosphate glasses by depolymerising the long phosphate chains as well as replaces the P-O-P bonds by more chemically durable bonds through the generation of non-bridging oxygen ions (NBO) (Wu *et al.*, 2016). Presence of MgO also tighten the glass network compared to CaO due to its high ionic field strength values (~ 5 Å^{-2}) and thereby enhances the glass mechanical strength and density (Diba *et al.*, 2012). Eventhough research on magnesium zinc-sulfophosphate glasses doped with RE ions is rather interesting however it is less explored and the mechanism of ligand interaction with RE ions is far from being understood (Da *et al.*, 2011).

In this study, a series of Nd^{3+}-doped magnesium zinc sulfophosphate glass systems are prepared. The Nd^{3+} ions concentration dependent absorbance, optical band gap, Urbach energy, density, molar volume, molar refractivity, refractive index and electronic polarizability are evaluated. The proposed glass system is

shown to be beneficial for the development of optical storage devices and solid state lasers.

MATERIALS AND METHODS

Six magnesium-zinc sulfophosphate glass samples of composition (60-*x*)P_2O_5-20MgO-20$ZnSO_4$-*x*Nd_2O_3 (where *x* = 0.5, 1.0, 1.5, 2.0 and 2.5 mol%) are synthesized using melt-quenching technique and labelled as PMZ*x*Nd. Analytical grade high-purity powders (from Sigma Aldrich chemicals, ~99.99%) of P_2O_5,MgO,$ZnSO_4 \cdot 7H_2O$ and Nd_2O_3 are used as the glass constituents. About 22 g of the batch composition is completely ground using an agate mortar, homogeneously mixed and placed into a alumina crucible, which is then heated at 300 °C for about 0.5 h to removed excess water and prevent excess boiling or consequent spillage. Then, the preheated glass constituent is completely melted in an electrical furnace at 1100 °C for 1.5 h. Upon reaching the desired viscosity, the transparent melt is poured into a stainless steel mould and annealed into another electric furnace at 300 °C for 3 h to release internal mechanical strain. After 3 h, the furnace is switched off and cool down to room temperature. Finally, the frozen solid samples are cut and polished to obtain good transparent surfaces required for optical measurements. The X-ray diffraction (XRD) patterns are recorded on a PANalytical X'Pert PRO MRD PW3040 diffractometer in scanning angle (2θ) range between 20° and 80° which used Cu Kα radiations (λ = 1.54 Å) operated at 40 kV and 35 mA. Optical absorption spectra in the wavelength range of 300–1000 nm are measured using a Shimadzu UVPC-3101 spectrophotometer. Glass density (ρ) is determined by Archimedes method with toluene (dendity ρ_t = 0.86669 g.cm^{-3}) as immersion media using the expression:

$$\rho = \frac{W_a}{W_a - W_t}\rho_t \tag{1}$$

where W_a and W_t are the weight of the glass sample in the air and inside toluene, respecyively. The molar volume (V_m) of glass sample in terms of molecular weight (M) yields:

$$V_m = \frac{M}{\rho} \tag{2}$$

The glass refractive inded (n) is calculated via (Dimitrov and Sakka, 1996) :

$$\frac{n^2-1}{n^2+2} = 1 - \sqrt{\frac{E_{opt}}{20}} \tag{3}$$

where E_{opt} is the optical band gap energy of the glass which is obtained from the UV absorption edge data. The molar refractivity (R_m) and polarizability (α_e) of the glass samples are estimated using the relations (Lorentz, 1880 ; Lorenz, 1880):

$$R_m = \frac{n^2-1}{n^2+2}(V_m) \tag{4}$$

$$\alpha_e = \frac{3}{4\pi}\left(\frac{R_m}{N_a}\right) \tag{5}$$

where N_a is the Avogadro's number. The optical band gap and Urbach energy (ΔE) in terms absorption coefficient $\alpha(\omega)$ yields:

$$\alpha(\omega) = \frac{B\left(\hbar\omega - E_{opt}\right)^r}{\hbar\omega} \tag{6}$$

$$\alpha(\omega) = B\exp\left(\frac{\hbar\omega}{\Delta E}\right) \tag{7}$$

where B is a constant, $\omega = 2\pi\upsilon$ is the angular frequency, $\hbar$ is the Planck constant divided by 2π and r is the transition index which is chosen as 1/2 for direct allowed transition and 2 for indirect allowed transition. Tauc plot ($(\alpha\hbar\omega)^{\frac{1}{r}}$ versus $\hbar\omega$) is generated to evaluate the value of E_{opt} . The reciprocal of the slope in the linear region of $\ln(\alpha)$ versus $\hbar\omega$ plot is used to compute the values of ΔE .

RESULTS AND DISCUSSION

XRD analysis

The XRD patterns of prepared glass without Nd_2O_3 and with optimum Nd_2O_3 concentration are shown in Fig.1. The absence of sharp peaks and presence of broad humps around 20-30° confirm the amorphous nature of prepared sample (Kaur, Preet, Singh, Devinder and Singh, 2016; Shan *et al.*, 2016). Absence of any crystallization peak corresponding to Nd^{3+} ions clearly indicate that these ions are completely entered into the glass matrix (Liang *et al.*, 2014).

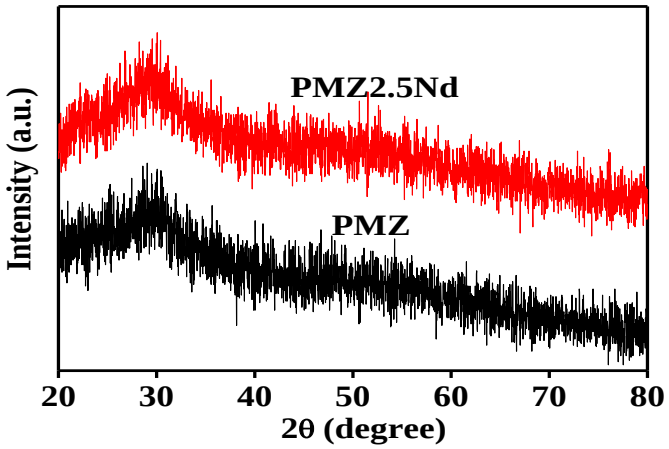

Fig. 1 XRD pattern of glass samples without Nd ions (PMZ) and with optimum Nd ions concentration (PMZ2.5Nd).

Physical properties

Table 1 enlists the physical properties of all sysnthesized glass samples including density, molar volume, refractive index, molar refractivity and electronic polarizability. Variations in the glass density signifies the alteration in glass network structure. Density is influenced by the structural compactness, change in the coordination of the glass-forming ions and the fluctuations in the dimensions of the interstitial holes (Elbashar *et al.*, 2016; Lakshminarayana *et al.*, 2017). Meanwhile, molar volume reflects changes in bond length that are responsible for the shrinking of the glass network structure *(Kaur, et al.*, 2016). The observed increase in the glass density from 2.62 to 2.77 g·cm^{-3} can be understood on the basis of molecular weight of oxides used for glass preparation. Since the molecular weight of Nd_2O_3 (336.48 g.mol^{-1}) is greater than P_2O_5 (141.94 g.mol^{-1}), the addition Nd_2O_3 at expense of P_2O_5 increases the density of glass (Pawar *et al.*, 2016). Furthermore, larger ionic radii of Nd^{3+} (1.163 Å) than P^{5+} (0.29 Å) (Shannon and Prewitt, 1969; Shannon, 1976) allow Nd^{3+} ions to fill most of the excess space volume and thereby enhance the glass network compactness (Ismail *et al.*, 2016). Generally, it is expected that the density and molar volume should show opposite behavior to each other (Samdani *et al.*, 2017). The interruption of glass network by neodymium interstices shortens the average P-oxygen distance and interatomic spacing (Jlassi *et al.*, 2016). This short interatomic spacing strengthen the interatomic forces between the modifying cations and the glass forming anions inside the network. Consequently, more compact and dense glass sample can be acheived (Pawar *et al.*, 2016; Matori *et al.*, 2017).

Refractive index is affected by the interaction of light with the electrons of the constituent atoms of the glass (Halimah *et al.*, 2017). It is related to the electronic polarization of the ions and the local field inside the glass. According to the electronic structure theory, the

performance of optical fibers is decided by the refractive index value (Lakshminarayana *et al.*, 2017). The increase of refractive index from range 1.85 to 1.90 with increasing Nd_2O_3 content is attributed to the increase of electronic polarizability (Melo *et al.*, 2016). The higher values of glass refractive index also reflect smaller band gap and more compact or regular network structure (Ismail *et al.*, 2016). Meanwhile, the observed increase in the molar refractivity and electronic polarizability with increasing Nd_2O_3 contents suggests that more numbers of non-bridging oxygen (NBOs) are generated in the glass matrix. It is known that NBOs have higher polarizability than bringing oxygen (BOs) (Halimah *et al.*, 2017). The present findings are in good agreement with other report (Azmi *et al.*, 2015).

Table 1 Physical properties of all prepared samples.

Sample	ρ (g.cm^{-3})	V_m (cm^3.mol^{-1})	n	R_m (cm^3)	α_e (x10^{-23})
PMZ	2.62	57.41	1.85	25.67	3.19
PMZ0.5Nd	2.63	57.64	1.85	25.79	3.21
PMZ1.0Nd	2.67	57.03	1.86	25.70	3.20
PMZ1.5Nd	2.75	55.79	1.90	26.03	3.24
PMZ2.0Nd	2.76	56.08	1.89	25.89	3.22
PMZ2.5Nd	2.77	56.25	1.90	26.30	3.27

Absorption properties

Fig. 2 shows the room temperature UV-Vis-NIR absorption spectra of the proposed glass system for different Nd_2O_3 concentrations. It consists of ten absorption bands which are located at 352, 428, 468, 522, 578, 622, 680, 742, 800 and 872 nm. These bands are corresponding to transitions in Nd^{3+} ion from the ground state $^4I_{9/2}$ to excited levels or manifolds (terms symbol of $^{2S+1}L_J$). These atomic terms in the orger of increaing absorption wavelengths include $^2D_{1/2}$+$^4D_{3/2}$, $^2P_{1/2}$, $^2D_{3/2}$+$^2G_{9/2}$, $^4G_{9/2}$+$^2K_{13/2}$, $^4G_{7/2}$, $^4G_{5/2}$, $^4H_{11/2}$, $^4F_{9/2}$, $^4F_{7/2}$+$^4S_{3/2}$, $^4F_{5/2}$+$^4H_{9/2}$ and $^4F_{3/2}$, respectively (Saddeek *et al.*, 2017).

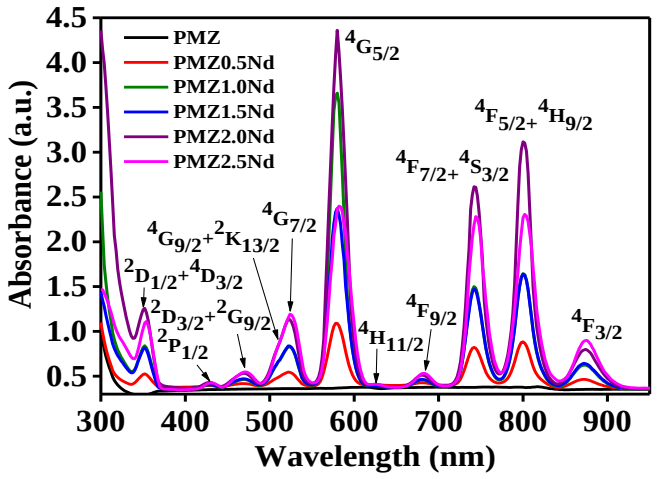

Fig. 2 Absorption spectra of prepared samples.

Due to the inhomogeneous broadening, the Stark structure of the Nd^{3+} J states is generally not resolved (Novais *et al.*, 2015). Overall, no obvious change in the position of absorption bands for different glass sample is evidenced. This is majorly ascribed to the shielding nature of 4f electrons by the outermost orbital. The absorbance is only affected by the surrounding ligand environment due to the variation of Nd^{3+} contents (Ratnakaram *et al.*, 2016). The absorbance of Nd^{3+} ion in the proposed glass system is higher compares to the system such as silica (Chimalawong *et al.*, 2010), germanate (Kassab *et al.*, 2016) and other phosphate containing diverse modifiers (Dantas *et al.*, 2013). It is worth noting that the concentration of Nd^{3+} ion (mol%) used in present work is much lower than the one previously used by others. This is attributed to character of the ion–host interaction in different glass system (Reddy Prasad *et al.*, 2016), where the nature of the ligand bonds available for the metal-central atom affect the energy of the absorption bands and thus results the glass colour (Träger, 2012).

The ligand effect cause the violet colour of sulfophosphate glass which originally colourless with incorporation of Nd^{3+} ions (Bach and Neuroth, 1998). Usually, metal centers coordinated by sulfur ligands may be primed for facilitation of an electron-transfer pathway to regenerate the active-absorption site. The closeness of metal and ligand orbital energies and their favorable overlap gives rise to the extensive electron delocalisation. The HOMO and LUMO states relevant to the electron transfer are clearly delocalized. Therefore, less energy is required to move the electron from ligand-based orbital to a metal-based orbital. This mechanism is responsible for the significant absorbance in the proposed glass system (Stiefel, 1996).

Optical band gap and urbach energy

Table 2 enlists the valued of optical band gap energy (E_{opt}) for direct (E_{dir}) and indirect (E_{ind}) transition as well as Urbach energy (ΔE). These optical band gap energies are used to characterize the lasing potential of the proposed glass system. It is achieved by analyzing the fundamental absorption edge data connected to the optical transitions and electronic band structure of the prepared amorphous structure (Kesavulu *et al.*, 2016). There are two types of optical band gap, which can occur at the fundamental absorption edge of crystalline and non-crystalline materials. For both direct and indirect optical band gap the electromagnetic waves interact with the electrons in the valence band before being raised to the conduction band across the fundamental gap. Glasses being amorphous have no well defined electronic conduction band. However, the existence of analogous optical conduction band is influenced by the glass forming anions. On top, the cations play indirectly a significant role (Kesavulu *et al.*, 2016; Nurhafizah *et al.*, 2016).

Table 2 Optical parameter of prepared samples.

Sample	E_{dir} (eV)	E_{ind} (eV)	ΔE (eV)
PMZ	3.86	3.79	0.28
PMZ0.5Nd	3.84	3.78	0.29
PMZ1.0Nd	3.82	3.71	1.91
PMZ1.5Nd	3.43	3.35	1.95
PMZ2.0Nd	3.46	3.46	1.83
PMZ2.5Nd	3.45	3.33	1.75

The estimated values of E_{opt} for E_{dir} is ranged between 3.79 to 3.33 and for E_{ind} it is ranged between 3.86 to 3.45 eV. Both of the optical band gap energy shows reduction with increasing concentration of Nd^{3+} ions. This reduction in E_{opt} is ascribed to the increase of polarizability or the generation of large number of NBOs and bonding defect due to the replacement of P^{5+} with Nd^{3+} ions (Kaur *et al.*, 2016; Nurhafizah *et al.*, 2016; Othman *et al.*, 2016; Zamratul *et al.*, 2016). This caused the broadening of the band tailing or impurity band which eventually merges with the bottom of the conduction band (Othman *et al.*, 2016; Zamratul *et al.*, 2016). The increase in degree of localization of electrons causes an enhancement of the donor centers in the glass network. The emergence of higher concentration of these donor centers reduces the optical band gap and shifts the absorption edge gradually towards higher wavelength. Therefore, more electrons can easily be transferred from the valence band to the conduction band (Ismail *et al.*, 2016; Kesavulu *et al.*, 2016).

The observed changes in the value of ΔE are related to the reorganization of the localized density of disordered states. These band tail arises due to the presence of impurities, structural defects and other inhomogenities in the host matrices (Selvi *et al.*, 2015). Urbach energy is increased from 0.28 to 1.95 eV. Higher value of ΔE indicates higher disorder in the glass matrix as the consequence of more extension of the localized states within the gap (Soltani *et al.*, 2016). Iniatially, Nd^{3+} doping up to 1.5 mol% into the glass cause disorders the glass system and then slightly drop indicating that the disorder in the localized states

decreased, yet not any greater than glass without additon Nd^{3+} ions. This indicate the glass started to become more stable and homogenous (Nurhafizah *et al.*, 2016). This result are in agreement with previous studies (Novais *et al.*, 2015).

CONCLUSION

A series of P_2O_5-MgO-$ZnSO_4$ glasses doped with different concentrations of Nd_2O_3 are synthesized via melt-quenching technique and characterized. The Nd^{3+} ions contents dependent physical and absorption features are determined. The indirect and direct optical band gaps are reduced from 3.79 to 3.33 eV and 3.86 to 3.45 eV, respectively. Conversely, both Urbach energy and refractive index are increased from 0.28 to 1.95 eV and 1.85 to 1.90 with increasing Nd_2O_3 contents. Furthermore, the physical parameters such as glass density, molar volume, molar refractivity and polarizability are found to be in the range of 2.62-2.77 $g{\cdot}cm^{-3}$, 56.25–57.41 $cm^3{\cdot}mol^{-1}$, 25.67–26.30 cm^3 and 3.19–3.17×10^{23}, respectively. Results revealed that the absorption and physical properties of the proposed sulfophosphate glass system can be improved by controlling the concentration of Nd_2O_3 which is advantageous for achieving potential laser-active medium.

ACKNOWLEDGEMENTS

This work was financially supported by the Universiti Teknologi Malaysia under the Research University Grant and Ministry of Higher Education Malaysia via vote 12H42 (GUP) , 13H50 (GUP) and 17H19 (GUP).

REFERENCES

Ahmadi, F., Hussin, R., and Ghoshal, S. K. 2016a. Judd-Ofelt intensity parameters of samarium-doped magnesium zinc sulfophosphate glass. *Journal of Non-Crystalline Solids*, 448, 43–51.

Ahmadi, F., Hussin, R., and Ghoshal, S. K. 2016b. Optical transitions in Dy^{3+}-doped magnesium zinc sulfophosphate glass. *Journal of Non-Crystalline Solids*, 452, 266–272.

Azmi, S. A. M., Sahar, M. R., Ghoshal, S. K., and Arifin, R. 2015. Modification of structural and physical properties of samarium doped zinc phosphate glasses due to the inclusion of nickel oxide nanoparticles. *Journal of Non-Crystalline Solids*, 411, 53–58.

Bach, H. and Neuroth, N. 1998. *The Properties of Optical Glass*. Springer. Mainz, 355–357.

Binnemans, K., Van Deun, R., Gorller-Walrand, C. and Adam, J. L. 1998. Optical properties of Nd^{3+}-doped fluorophosphate glasses. *Alloys and Compounds*, 275-277, 455–460.

Chimalawong, P., Kaewkhao, J., and Limsuwan, P. 2010. Effect of Nd^{3+} concentration on the physical and absorption properties of soda-lime-silicate glasses. *Advanced Materials Research*, 93-94, 455–458.

Da, N., Peng, M., Krolikowski, S., and Wondraczek, L. 2010a. Intense red photoluminescence from Mn^{2+}-doped (Na^+; Zn^{2+}) sulfophosphate glasses and glass ceramics as LED converters. *Optics Express*, 18, 2549–2557.

Da, N., Krolikowski, S., Nielsen, K. H., Kaschta, J., and Wondraczek, L. 2010b. Viscosity and softening behavior of alkali zinc sulfophosphate glasses. *Journal of the American Ceramic Society*, 93, 2171–2174.

Da, N., Grassme, O., Nielsen, K. H., Peters, G., and Wondraczek, L. 2011. Formation and structure of ionic (Na, Zn) sulfophosphate glasses. *Journal of Non-Crystalline Solids*, 357, 2202–2206.

Dantas, N. O., Serqueira, E. O., Silva, A. C. A., Andrade, A. A., and Lourenço, S. A. 2013. High quantum efficiency of Nd^{3+} ions in a phosphate glass system using the Judd-Ofelt theory. *Brazilian Journal of Physics*, 43, 230–238.

Diba, M., Tapia, F., Boccaccini, A.R., and Strobel, L. A. 2012. Magnesium-containing bioactive glasses for biomedical applications. *International Journal of Applied Glass Science*, 3, 221–253.

Dimitrov, V. and Sakka, S. 1996. Linear and nonlinear optical properties of simple oxides. II. *Journal of Applied Physics*, 79, 1741-1745.

Dorosz, D. 2008. Rare earth ions doped aluminosilicate and phosphate double clad optical fibres. *Bulletin of the Polish Academy of Sciences Technical Sciences*, 56, 103–111.

Ehrmann, P. R. and Campbell, J. H. 2002. Nonradiative energy losses and radiation trapping in neodymium-doped phosphate laser glasses. *Journal of the American Ceramic Society*, 85, 1061–1069.

Elan, F., Falcao-Filho, E. L., Camilo, M. E., Garcia, J. A. M., Kassab, L. R. P., and de Araujo, C.B. 2016. Upconversion photoluminescence in GeO_2-PbO glass codoped with Nd^{3+} and Yb^{3+}. *Optical Materials*, 60, 313–317.

Elbashar, Y. H., Ali, M. I., Elshaikh, H. A., and El-Din Mostafa, A. G. 2016. Influence of CuO and Al_2O_3 addition on the optical properties of sodium zinc phosphate glass absorption filters. *Optik*, 127, 7041–7053.

Griscom, L. S., Balda, R., Mendioroz, A., Smektala, F., and Fern, J. 2001. Up-conversion processes in Nd^{3+}-doped chloro-sulfide glasses. 284, 268–273.

Halimah, M. K., Faznny, M. F., Azlan, M. N., and Sidek, H. A. A. 2017. Optical basicity and electronic polarizability of zinc borotellurite glass doped La^{3+} ions. *Results in Physics*, 3–11.

Hu, L., Chen, S., Tang, J., Wang, B., Meng, T., Chen, W., Wen, L., Hu, J., Li, S., Xu, Y., Jiang, Y., Zhang, J., and Jiang, Z. 2014. Large aperture N31 neodymium phosphate laser glass for use in a high power laser facility. *High Power Laser Science and Engineering*, 2, 1–6.

Ismail, S. F., Sahar, M. R., and Ghoshal, S. K. 2016. Physical and absorption properties of titanium nanoparticles incorporated into zinc magnesium phosphate glass. *Materials Characterization*, 111, 177–182.

Jlassi, I., Elhouichet, H., and Ferid, M. 2016. Influence of Mgo on structure and optical properties of alumino-lithium-phosphate glasses. *Physica E: Low-Dimensional Systems and Nanostructures*, 81, 219–225.

Kassab, L.R., Silva, D.M., Garcia, J.A., da Silva, D.S. and de Araújo, C.B., 2016. Silver nanoparticles enhanced photoluminescence of Nd^{3+} doped germanate glasses at 1064 nm. *Optical Materials*, 60, 25–29.

Kaur, Preet, Singh, Devinder and Singh, T. 2016. Optical, Photoluminescence and physical properties of Sm^{3+} doped lead alumino phosphate glasses. *Journal Of Non-Crystalline Solids*, 452, 87–92.

Kesavulu, C.R., Kim, H.J., Lee, S.W., Kaewkhao, J., Wantana, N., Kaewnuam, E., Kothan, S., and Kaewjaeng, S. 2016. Spectroscopic investigations of Nd^{3+} doped gadolinium calcium silica borate glasses for the NIR emission at 1059 nm. *Journal of Alloys and Compounds*.

Lakshminarayana, G., Kaky, K. M., Baki, S. O., Lira, A., Nayar, P., Kityk, I. V., and Mahdi, M. A. 2017. Physical, structural, thermal, and optical spectroscopy studies of TeO_2-B_2O_3-MoO_3-ZnO-R_2O (R=Li, Na, and K)/MO (M=Mg, Ca, And Pb) glasses. *Journal of Alloys and Compounds*, 690, 799–816.

Liang, X., Li, H., Wang, C., Yu, H., Li, Z., and Yang, S. 2014. Physical and structural properties of calcium iron phosphate glass doped with rare earth. *Journal of Non-Crystalline Solids*, 402, 135–140.

Lorentz, H. A. 1880. *Über die Beziehung zwischen der Fortpflan zungsgeschwindigkeit des Lichtes und der Körperdichte* [On the relation between the propagation speed of light and density of a body], Annals of Physics, 9, 641-665. DOI: 10.1002/andp.18802450406

Lorenz, L. 1880. *Über die Refractionsconstante* [About the constant of refraction], Annals of Physics, 11, 70-103. DOI: 10.1002/andp. 18802470905.

Matori, K. A., Sayyed, M.I., Sidek, H. A. A., Zaid, M.H.M., and Singh, V.P. 2017. Comprehensive study on physical, elastic and shielding properties of lead zinc phosphate glasses. *Journal of Non-Crystalline Solids*, 457, 97–103.

Melo, G. H. A, Dias, J. D. M., Lodi, T. A., Barboza, M. J., Pedrochi, F., and Steimacher, A. 2016. Optical and spectroscopic properties of Eu_2O_3 doped CaBaAl glasses. *Optical Materials*, 54, 98–103.

Miguel, A., Azkargorta, J., Morea, R., Iparraguirre, I., Gonzalo, J., Fernandez, J., and Balda, R. 2013. Spectral study of the stimulated emission of Nd^{3+} in fluorotellurite bulk glass. *Opt Express*, 21, 9298–9307.

Novais, A. L. F., Dantas, N. O., Guedes, I., and Vermelho, M. V. D. 2015. Spectroscopic properties of highly Nd-doped lead phosphate glass. *Journal of Alloys and Compounds*, 648, 338–345. Elsevier B.V.

Nurhafizah, H., Rohani, M. S., and Ghoshal, S. K. 2016. Er^{3+}:Nd^{3+} concentration dependent spectral features of lithium-niobate-tellurite amorphous media. *Journal of Non-Crystalline Solids*, 443, 23–32.

Othman, Arzumanian, and Möncke, D. 2016. The influence of different alkaline earth oxides on the structural and optical properties of undoped, Ce-doped, Sm-doped, and Sm/Ce co-doped lithium alumino-phosphate glasses. *Optical Materials.* 1-8.

Pawar, P. P., Munishwar, S. R., and Gedam, R. S. 2016. Intense white light luminescent Dy^{3+} doped lithium borate glasses for w-LED: A correlation between physical, thermal, structural and optical properties. *Solid State Sciences*, 64, 41–50.

Ratnakaram, Y. C., Babu, S., Bharat, L. K., and Nayak, C. 2016. Fluorescence characteristics of Nd^{3+} doped multicomponent fluoro-phosphate glasses for potential solid-state laser applications. *Journal of Luminescence*, 175, 57–66.

Reddy Prasad, V., Seshadri, M., Babu, S., and Ratnakaram, Y. C. 2016. Concentration-dependent studies of Nd^{3+}-doped zinc phosphate glasses for

nir photoluminescence at 1.05 μm. *Journal of Biological and Chemical Luminescence*.1-9.

Saddeek, Y. B., El-Maaref, A. A., Aly, K. A., ElOkr, M. M., and Showahy, A. A. 2017. Investigations on spectroscopic and elasticity studies of Nd_2O_3 doped CANP phosphate glasses. *Journal of Alloys and Compounds*, 694, 325–332.

Samdani, Ramadevudu, G., Chary, M. N., and Shareefuddin, M. 2017. Physical and spectroscopic studies of Cr^{3+} doped mixed alkaline earth oxide borate glasses. *Materials Chemistry and Physics*, 186, 382–389.

Selvi, S., Marimuthu, K., and Muralidharan, G. 2015. Structural and luminescence behavior of Sm^{3+} ions doped lead boro-telluro-phosphate glasses. *Journal of Luminescence*, 159, 207–218.

Shan, X., Tang, G., Chen, X., Peng, S., Liu, W., Qian, Q., Chen, D., and Yang, Z. 2016. Silver nanoparticles enhanced near-infrared luminescence of Er^{3+}/Yb^{3+} Co-doped multicomponent phosphate glasses. *Journal of Rare Earths*, 34, 868–875.

Shannon, R. D. 1976. Revised effective ionic radii and systematic studies of interatomic distances in halides and chalcogenides. *Acta Crystallographica Section A*, 32, 751–767.

Shannon, R. D. and Prewitt, C. T. 1969. Effective ionic radii in oxides and fluorides. *Acta Crystallographica Section B Structural Crystallography and Crystal Chemistry*, 25, 925–946.

Soltani, I., Hraiech, S., Horchani-Naifer, K., Elhouichet, H., Gelloz, B., and Férid, M. 2016. Growth of silver nanoparticles stimulate spectroscopic properties of Er^{3+} doped phosphate glasses: Heat treatment effect. *Journal of Alloys and Compounds*, 686, 556–563.

Stiefel, E. I. 1996. Transition metal sulfur chemistry: biological and industrial significance and key trends. *American Chemical Society*, 1–37.

Striepe, S., Da, N., Deubener, J., and Wondraczek, L. 2012. Micromechanical properties of (Na,Zn)-sulfophosphate glasses. *Journal of Non-Crystalline Solids*, 358, 1032–1037.

Surana, S. S. L., Sharma, Y. K., and Tandon, S. P. 2001. Laser action in neodymium-doped zinc chloride borophosphate glasses. *Materials Science and Engineering B: Solid-State Materials for Advanced Technology*, 83, 204–209.

Thieme, A., Möncke, D., Limbach, R., Fuhrmann, S., Kamitsos, E. I., and Wondraczek, L. 2015. Structure and properties of alkali and silver sulfophosphate glasses. *Journal of Non-Crystalline Solids*, 410, 142–150.

Träger, F. 2012. *Handbook of Lasers and Optics*. Springer. Kassel, p. 1332.

Wu, F., Li, S., Chang, Z., Liu, H., Huang, S., and Yue, Y. 2016. Local structure characterization and thermal properties of P_2O_5-MgO-Na_2O-Li_2O glasses doped with SiO_2. *Journal of Molecular Structure*, 1118, 42–47.

Zamratul, M. I. M., Zaidan, A. W., Khamirul, A. M., Nurzilla, M., and Halim, S. A. 2016. Formation, structural and optical characterization of neodymium doped-zinc soda lime silica based glass. *Results in Physics*, 6, 295–298.